

Article Info

Received: 18 Aug 2018 | Revised Submission: 28 Aug 2018 | Accepted: 02 Sept 2018 | Available Online: 15 Sept 2018

A Statistical Analysis of Corrosion Rate and Mechanical Properties of Metal Inert Gas Welding

Ibraheem Sabry and Ahmed M El-Kassas***

ABSTRACT

In the present work an attempt has been made to optimize the process parameters of metal inert gas welding for aluminum pipes 6061 to evaluate the output quality characteristics using factorial design. An interaction effect of input parameters is also studied to predict their influence on the output response. The performance of MIG for aluminum pipe is evaluated in terms of joint's tensile strength and corrosion rate, factorial design technique has been employed using orthogonal array, ANOVA (analysis of variance) to study contribution of each parameter and interaction of them on output and confirmation tests at 95 % confidence level to compare with experimental results. Optimal combination of parameters is presented with a good agreement found between the estimated and experimental results within the preferred significant level after verifying experimentally. It was confirmed that factorial design with ANOVA and confirmation tests successfully improved the quality characteristics of tensile strength and corrosion rate of MIG process.

Keywords: Corrosion Rate; Tensile Strength; MIG; ANOVA.

1.0 Introduction

Aluminium can't successfully be arc welded in an air environment, due to the affinity for oxygen. If fusion welded in normal atmosphere oxidizes readily happens and this outcome in both slag inclusion and porosity in the weld, greatly reducing its mechanical properties. In modern years, there has been a potential demand for lightweight transport equipment. The use of aluminum alloys to substitution ferrous alloys in transport equipment is most effective in reducing the weight of automobiles and aerospace vehicles. Considerable tonnages of aluminum alloys are used in the transport manufacture. In that esteem, the strength to weight ratios of aluminum alloys has thus been a predominant design consideration. Several strengthening mechanisms have been used in the else 30 years to incubate new aluminum alloys with high strength to weight ratios.

Stampede hardening, precipitation hardening, and improvement of grain structure provide active strengthening mechanisms [1-2]. Fusion welding of mercantile aluminum alloys is mostly hard and not bespoke for some aluminum alloy groups. The existence of protective tenacious oxide film on aluminum alloys is accountable for such difficulties.

Extensive sur-face planning to take off the oxide film is needful before welding of some aluminum alloys. Fusion welding of Al-alloys, whilst, faces some other problems, such as, generation of welding defects such as blowholes, cracks, welding distortion, and angular distortion, which reduced the mechanical properties of weldments. Fusion welding of high strength Al-alloys caused significant changes in the microstructure of cold worked and age hardened alloys, which drastically decrease the mechanical properties of welded alloys [3-4].

In this studied comparison friction stir welds with metal inert gas and tungsten inert gas through effect welding speed.

They also have been scrupulous to locate whether the fatigue strength of FS welds is affected by the welding speed, and also to contrast the fatigue outcome with the outcome for traditional arc welding methods: MIG pulse and TIG. The Al 6082 was FS welded in the temper conditions, and MIG-pulse and TIG welded in T6. The experimental outcome has been acquired that the fatigue strength of FS welded Al 6082 is higher than that of metal inert gas pulse and tungsten inert gas welds of the same material. The tungsten inert gas welds display best fatigue execution than metal inert gas welding [5].

*Corresponding Author: Department of Production Engineering, Modern Academy for Engineering & Technology, Egypt (E-mail: ibraheem.sabry@yahoo.com)

**Department of Production Engineering, Faculty of Engineering, Tanta University, Egypt

To relieve hot cracking in weldments of AA6061, Si-rich filler metals such as the joint ER4043 is mostly used [5-6]. This type of cracking is found to happen to rely on filler composition and mitigation [5]. Krishna P.Murali, Prasad and Ramanaiah et al. [18] [8] establish that longitudinal cracking happen when AA6061 was welded with Mg-rich filler metal ER5356 but not with Si-rich filler metal ER4043. Si- rich filler metals have also shown to block the build-up of brittle intermetallic compound (IMC) layer, and minimizing its thickness [7]. Numerous papers have been behave on ER5356 and ER4043 filler metals, since both are the generality joint filler metals to be used when welding AA6061 sheets.

In addendum, Song et al. [9] have communicate that filler metals such as ER4047 which possess completely similar installation could competitor the output quality of ER4043 . However, acquaintance on the belongings of alternate filler metals such as ER4047 on the AA6061 weldment is unusual. in based on the above literature the work on MIG for pipes are very little, This paper is centering on the effects that in mechanical properties and corrosion rate of welded Aluminum 6061 pipe using metal inert gas of filler weld material ER4043.

2.0 Expermintal Work

2.1 Selecting important mig process parameters

Based on preliminary trials, the independent process parameters affecting the ultimate tensile strength (UTS) and corrosion rate were identified as ampere (A), volt (V) and weld speed (S).

2.2 Selecting limits of mig process variable

The chemical composition and mechanical properties of Al 6061 aluminum alloys cylindrical parts used in the present study as delivered by the Miser Aluminum company are given in Tables (1-2). Using filler weld material ER4043 are used in the study.

The metal inert gas welding parameters are shown in the following Table (4) and the chemical composition of filler metal show in Table (3)[13]. Trial runs were conducted to find the upper and lower limit of process parameters for 6061 aluminum alloy, by varying one of the parameters and keeping the rest of them at constant values. The chemical composition and mechanical properties of the materials 6061.

Table 1: Chemical Composition (weight %) of Al6061

Weight %	Si	Fe	Cu	Mn	Mg	Cr	Zn	Ti
6061	0.4	0.70	0.15	0.15	0.9	0.04	0.25	0.15

Table 2: Mechanical Properties of Al6061

Alloy	σ UTS M pa	EL%	VHD
6061	252.690	8	86

Table 3: Chemical Composition (wt %) of Filler Material

Filler	Si	Mg	Cu	Fe	Mn	Zn	Ti
ER4043	5.0	0.005	0.3	0.8	0.05	0.1	0.2

are presented in Tables 1 and 2, respectively. Feasible limits of the parameters were chosen in such a way that the joint should be free from visible defects. The upper limit of a factor was coded as 1 and lower limit as -1.

The intermediate coded values are calculated from the following relationship:

$$Y = b_0 + b_1X + b_2Q + b_3Z + b_{11}X^2 + b_{22}Q^2 + b_{33}Z^2 + b_{12}QX + b_{13}QZ + b_{23}XZ \quad (1)$$

Where b_1, b_2 and b_3 are linear terms, b_{12}, b_{13} and b_{23} are interactive terms, b_{11}, b_{22} and b_{33} are the quadratic terms of the polynomial The coefficients b_0, b_1, b_2, b_3 and are the least square estimates of true polynomial, representing the response surface.

The strength of the respective process parameters and their interactions are represented by these coefficients.

The p value of regression analysis indicates the linear, square and interaction of the MIG process parameters with the response functions and these p values are used to identify the significant parameters on the response functions [16]. The selected process parameters with their limits, units and notations are given in Table 4.

2.3 Development of design matrix

The selected design matrix is shown in Table 5. It is a three factor three level central composite rotatable design consisting of 27 sets of coded conditions composed of a full factorial $2^4 = 16$, plus 6 centre points and 5 star points.

Table 4: Process Parameters and Their Levels in Metal Inert Gas

Process Parameters	Unit	Symbol	Levels		
			-1	0	1
Ampere	A	A	105	110	115
volt	V	v	17	18	19
Weld speed	mm/min	S	3	4	5

2.4 Conducting experiment as per design matrix

The experiments were conducted as per the design matrix with the help of MIG machine made by sonscn 400 machine. The pipe to be welded and electrode were 4043 show in Figure 2. Samples of the welded pipe are shown in Figure 1. Specimens of required size were cut from the welded pipe to carry out metallurgical studies.

Fig. 1: Sample of MIG Welded pipe (3 mm/min)



2.5 Recording of responses

Tensile test specimens were prepared as per American Society for Testing of Materials (ASTM E8) standard and transverse tensile properties such as ultimate tensile strength of the MIG welded joints were evaluated using computerized universal testing machine. For each welded pipe, three specimens were prepared and tested. The average values of the results obtained from those specimens are tabulated and presented in Table 5 as experimental value. Specimens for corrosion tests were fabricated with dimensions according to ASTM specifications for all metals used. using Potentiostat apparatus for polarization testtesting machine. After completing the fabrication of specimens, these specimens were categorized and sorted into groups and hardness values.

Fig 2: The tensile test Sample Geometry.

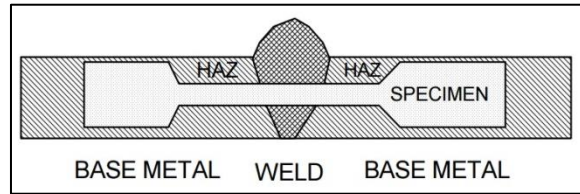
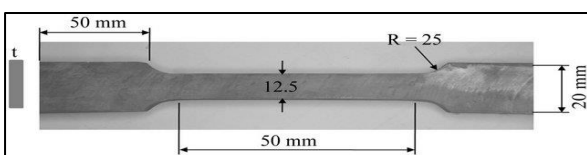


Fig.3: Photos of Sample Tensile Test Specimens



Table 5: Design matrix and experimental value with Predicted value of tensile strength and corrosion rate

Run	MIG process parameter			Tensile strength		Corrosion rate	
	A	V	S	Exp.	Pred.	Exp.	predicted
12	1	1	-1	115.22	115.82	0.004	0.025
16	1	1	-1	158.17	158.66	0.008	0.022
18	1	-1	-1	126.89	127.66	0.010	0.032
26	-1	-1	1	143.53	141.66	0.005	0.034
5	-1	1	1	136.70	137.21	0.009	9.1E-003
22	1	-1	-1	152.34	151.66	0.017	0.028
9	-1	1	-1	128.89	128.85	0.006	0.017
10	1	-1	1	144.50	143.83	0.009	0.018
14	1	-1	-1	137.70	136.77	0.019	0.024
24	-1	1	-1	122.06	121.66	0.020	0.036
11	-1	-1	-1	128.86	129.38	0.022	0.021
19	1	-1	1	144.50	144.02	0.025	0.025
4	0	0	0	151.34	152.16	0.020	5.8E-003
15	-1	1	-1	123.06	122.46	0.024	0.029
8	-1	-1	-1	142.53	143.66	0.028	0.010
25	1	1	1	156.17	157.85	0.024	0.030
23	1	1	-1	135.70	136.21	0.026	0.031
7	0	0	0	161.17	159.35	0.029	6.0E-003
20	-1	-1	1	128.86	129.32	0.025	0.027
13	1	1	1	151.34	151.96	0.026	0.021
21	-1	1	1	115.22	115.52	0.030	0.031
2	1	-1	1	128.86	129.32	0.026	7.0E-003
17	-1	1	1	143.53	142.72	0.029	0.026
3	0	0	0	117.22	116.02	0.040	0.012
1	1	1	1	143.50	143.52	0.030	4.7E-003
27	-1	-1	1	125.89	126.35	0.035	0.040
6	-1	-1	-1	123.06	123.16	0.040	0.015

3.0 Result and Discussion

3.1 Development of mathematical model

Ultimate tensile strength and corrosion rate of the MIG joints is function of ampere, welding speed and volt, and it can be expressed as

$$Y = f(A, S, V) \quad (2)$$

where Y is the response; A is the ampere, A; S is the welding speed, mm/s; V is the volt, v. For the three factors, the selected polynomial could be expressed as

$$Y = b_0 + b_1A + b_2V + b_3S + b_{11}A^2 + b_{22}V^2 + b_{33}S^2 + b_{12}AS + b_{13}AV + b_{23}VS \quad (2)$$

Where b_0 is the free term of the regression equation; the coefficients b_1 , b_2 and b_3 are linear terms; the coefficients b_{11} , b_{22} and b_{33} are quadratic terms; the coefficients, b_{12} , b_{13} and b_{23} , are interaction terms. The values of the coefficient of the polynomial are calculated by regression analysis with the help of following equations [12].

3.1.1 Design expert

8.0.4 software packages were used to calculate the values of those coefficients for different responses and the results are presented in Table 6. The final mathematical models determined by the above analysis in the coded form are represented.

Table 6: Calculated Regression Coefficients of Mathematical Models

Factor	Coefficient (tensile strength)	Coefficient (corrosion rate)
Intercept	-307.85370	+0.43637
A	+10.78902	+4.44444E-005
V	-13.25011	-0.061000
S	+15.44444	+0.022000
A ²	-0.028889	-1.77778E-005
V ²	+0.44444	+1.22222E-003
S ²	-0.055556	-3.77778E-003
SA	-0.10000	+2.00000E-004
SV	-0.25000	-1.66667E-004
AV	-0.15000	+2.00000E-004

The p value of regression analysis indicates the linear, square and interaction of the MIG process parameters with the response functions and these p values are used to identify the significant parameters on the response functions [16].

3.2 Checking the adequacy of the developed models using anova

The adequacy of the model developed was then tested by using the analysis of variance technique (ANOVA). The results for tensile strength

of the ANOVA are given in Table 7. The Model Fvalue of 462.24 for tensile strength implies the model is significant. There is only a 0.01% chance that a Model Fvalue could occur due to noise. Values of "Prob > F" less than 0.050 0 indicate that model terms are significant. In this case, N², S² and F² are significant model terms. Values greater than 0.100 0 indicate that the model terms are not significant. The lack of Fit Fvalue of 0.83 implies that the lack of fit is not significant. There is 57% chance that a lackof Fit Fvalue could occur due to noise. The coefficient of determination R² values gives the goodness of fitness of the model.

The results for corrosion rate of the ANOVA are given in Table 8. The Model Fvalue of 80.74 for corrosion rate implies the model is significant. There is only a 0.01% chance that a Model Fvalue could occur due to noise. Values of "Prob > F" less than 0.050 0 indicate that model terms are significant. In this case, N², S² and F² are significant model terms. Values greater than 0.100 0 indicate that the model terms are not significant. The lack of Fit Fvalue of 0.71 implies that the lack of fit is not significant. There is 50% chance that a lackof Fit Fvalue could occur due to noise. The coefficient of determination R² values gives the goodness of fitness of the model.

The determined values of the developed model are presented in Table 9. The R² value is always between 0 and 1, and its value indicates the accuracy of the model. For a good model, R² value should be close to 1. In this model, the calculated R² is 0.9771. This implies that 97.7% of experimental data confirms the compatibility with the data predicted by the developed model. The value of the adjusted R² of 0.965 15 is also high to adherent for a high significance of the model. The predicted R² of 0.9426 is in reasonable agreement with the adjusted R² of 0. 9426. Adequate precision measures the signaltonoise ratio. A ratio greater than 4 is desirable [13]. In this study, the ratio is 30.439, which indicates an adequate signal.

The determined values of the developed model are presented in Table 9. The R² value is always between 0 and 1, and its value indicates the accuracy of the model. For a good model, R² value should be close to 1. In this model, the calculated R² is 0.9771. This implies that 97.7% of experimental data confirms the compatibility with the data predicted by the developed model. The value of the adjusted R²

of 0.965 15 is also high to adherent for a high significance of the model. The predicted R 2 of 0.9426 is in reasonable agreement with the adjusted R 2 of 0. 9426. Adequate precision measures the signaltonoise ratio. A ratio greater than 4 is desirable [13]. In this study, the ratio is 30.439, which indicates an adequate signal.

Fig 3: Normal Probability Plot for Tensile Strength

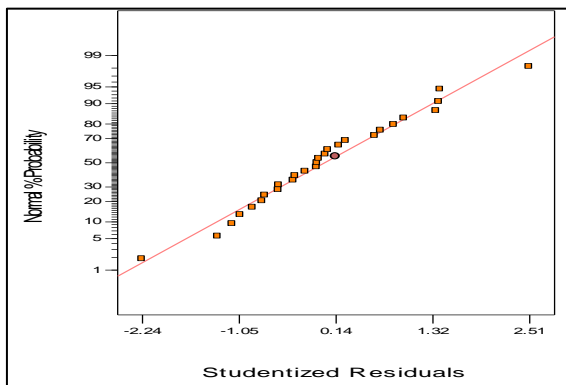
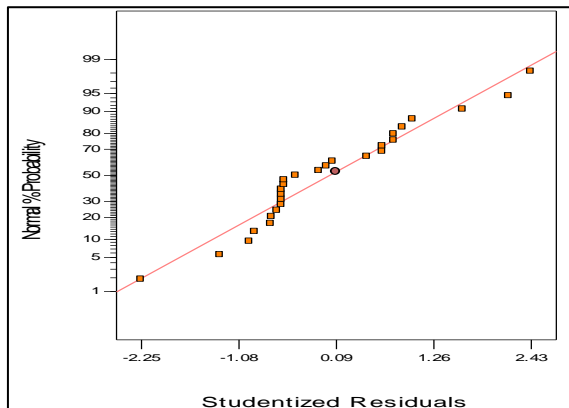


Fig 4: Normal probability Plot for Corrosion Rate



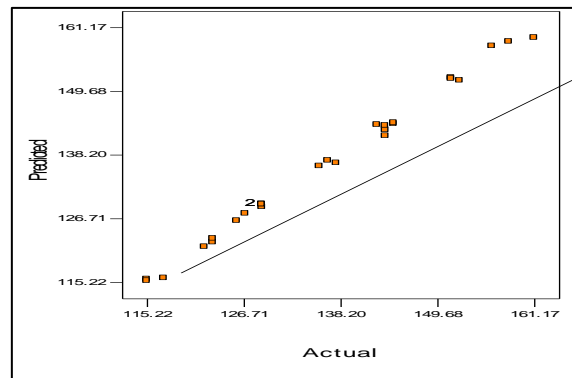
Distributed normally. A typical scatter diagram of the model is presented in Figure 3 and in Figure 4. The observed values and predicted values of the responses are scattered close to the 45° line, indicating an almost perfect fit of the developed empirical models

3.3 Confirmation experiments

Experiments are conducted to verify the regression equation .Three weld runs are made using different values of rotational speed, welding speed and axial force other than those used in the design matrix.

The results obtained are quite satisfactory and the details are presented in figure5 the relation between experimental tensile strength (actual) and predicted tensile strength. The results obtained

Fig. 5:Scatter Diagram of Ultimate Tensile Strength (UTS)



are quite satisfactory and the details are presented in figure 6 the relation between experimental corrosion rate (actual) and predicted corrosion rate.

3.4 Effect of mig process parameter

Tensile strength of MIG welded aluminum alloy 6061 pipes were predicted by the mathematical models using the experimental observations presented in Figures 7–12, showing the general trends between cause and effect. From Figures 7 and 9, it is seen that as the ampere increases the tensile strength of MIG welded aluminum alloy 6061 increases and then it decreases.

It is clear that in MIG as the ampere increases, the heat input also increases. More amount of heat input affects the regular flow behavior of the material. At the same time, low ampere produces low heat input, which results in the lack of stirring action, hence the strength is low. From Figures 7 and 11, it is evident that as welding speed increases from 3 mm/min to 5 mm/min, the tensile strength of the MIG welded aluminum alloy 6061 increases and then decreases. At the lowest welding speed (3 mm/min) and highest welding speed (5 mm/min), lower tensile strength is observed. This is due to the increased ampere and decreases voltage and insufficient heat generated respectively [14]. From Figures 9 and 11, it is observed that when the ampere increases from 105 to 115 the tensile strength of the MIG weld of 6061 increases and then decreases. This may be due to

insufficient coalescence of transferred material. 6061 increases and then decreases. This may be due to insufficient coalescence of transferred material.

Fig 6 : Scatter Diagram of Corrosion rate

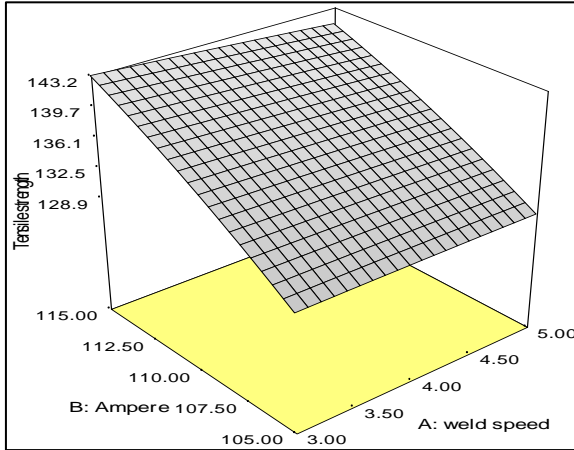


Fig 7: Response Surface Graphs of Ampere and Welding Speed On UTS

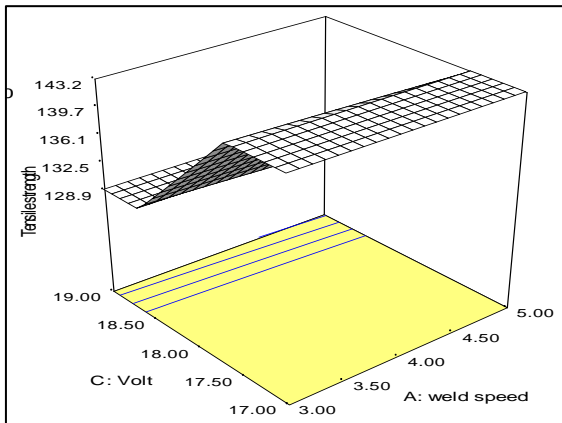


Fig 8: Contour Plots of Ampere Speed and Weld Speed Speed on UTS

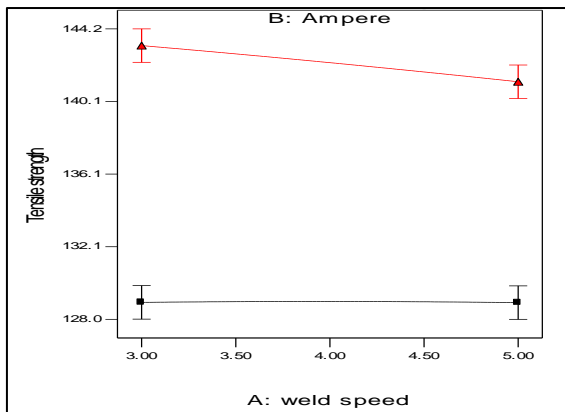


Fig 9: Response Surface Graphs of Volt and Weld Speed on UTS

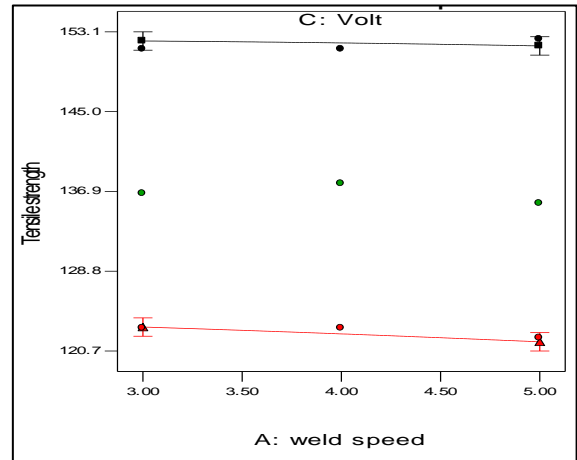


Fig 10: Contour Plots of Volt Speed and Weld Speed on UTS

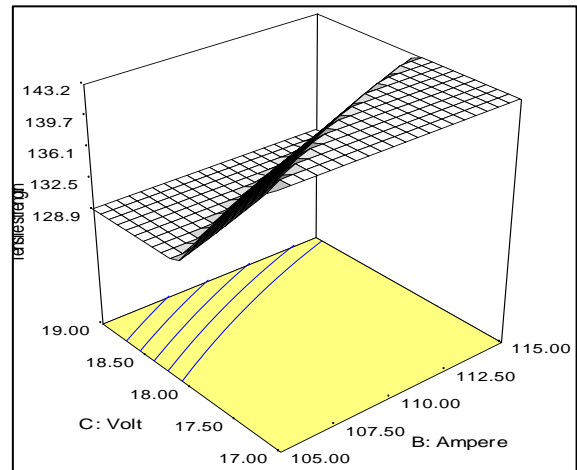


Fig 11: Response Surface Graphs of Ampere and Volt on UTS

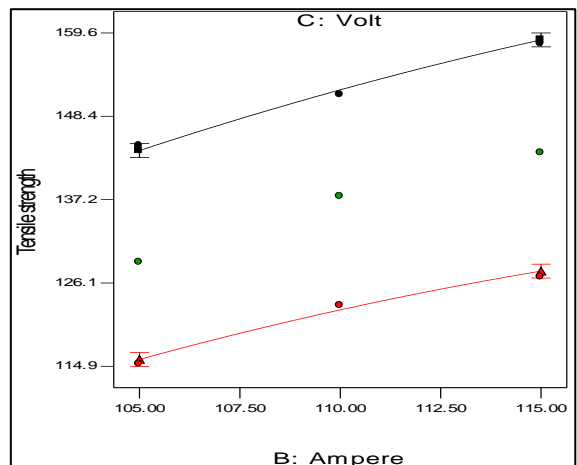


Fig 12 : Contour plots of Amperte and Volt on UTS

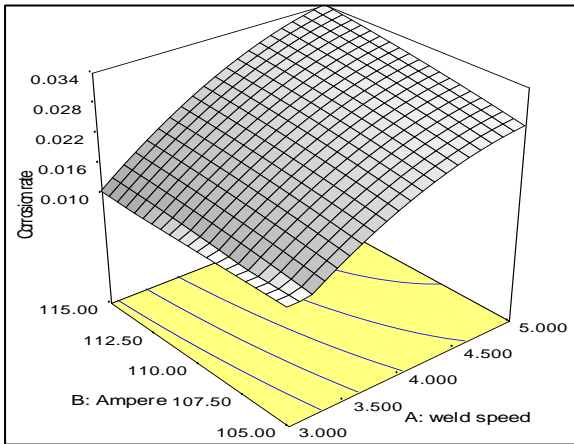


Fig 13 :Response Surface Graphs of Weld Speed and Ampere on Corrosion Rate

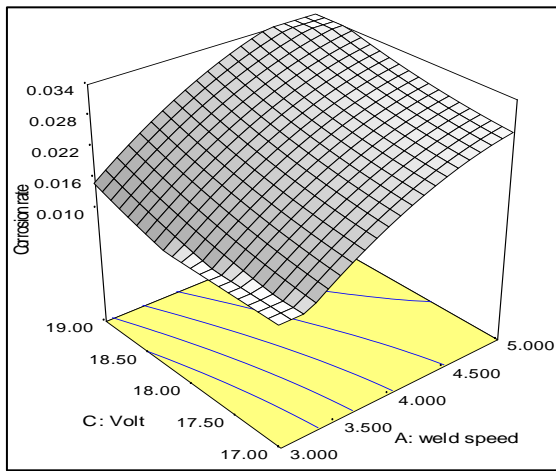


Fig 14: Response Surface Graphs of Ampere And Welding Speed on Corrosion Rate

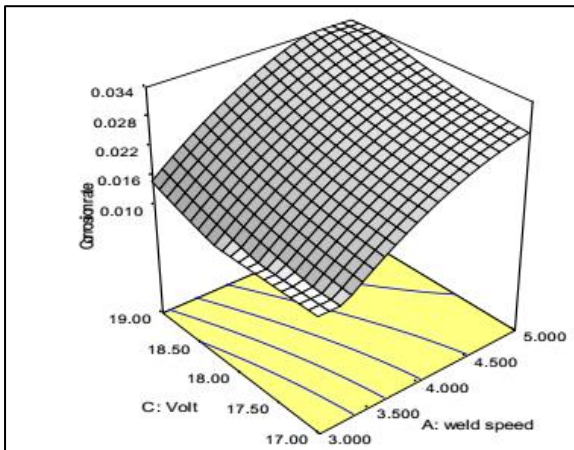


Fig 15: Response Surface Graphs of Volt and Welding Speed on Corrosion Rate

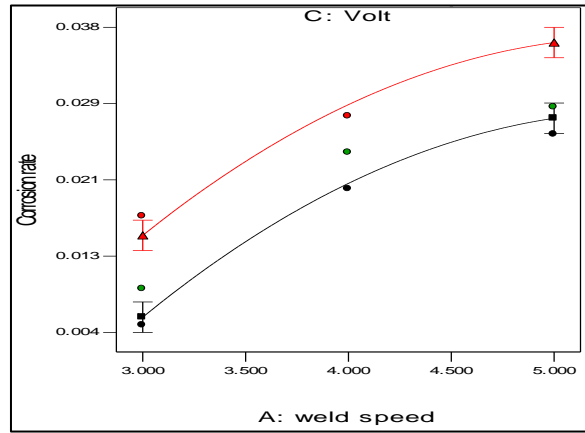


Fig 16: Response Surface Graphs of Volt And Welding Speed on Corrosion Rate

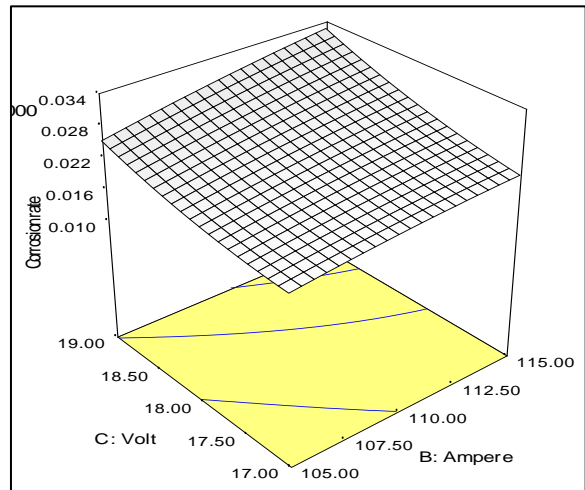


Fig 17:Response Surface graphs of Volt and Ampere on Corrosion Rate

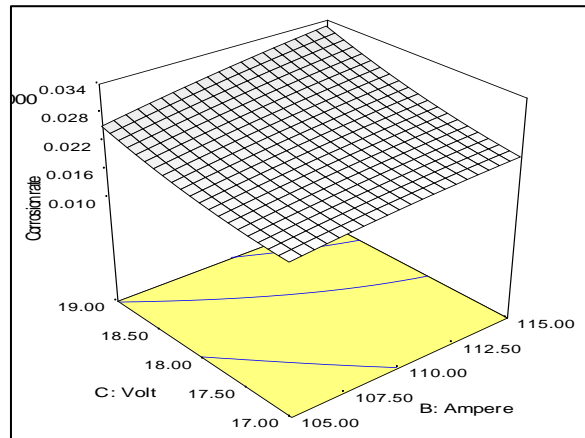


Table 7: ANOVA Test Results for Tensile Strength

Sources	Sum of Squares	DF	Mean Square	F Value	Prob > F	Result
Model	4735.68	9	526.19	462.24	< 0.0001	significant
S	1.39	1	1.39	1.22	0.2847	
A	539.11	1	539.11	473.59	< 0.0001	
V	2896.61	1	2896.61	2544.58	< 0.0001	
S ²	0.019	1	0.019	0.016	0.9000	
A ²	3.13	1	3.13	2.75	0.1156	
V ²	1.19	1	1.19	1.04	0.3219	
SA	3.00	1	3.00	2.64	0.1229	
SV	0.75	1	0.75	0.66	0.4282	
AV	6.75	1	6.75	5.93	0.0262	
Residual	19.35	17	1.14			
Lack of fit		17		0.83		Not significant
Pure error		0				
Cor Total	4755.03	26				

Fig 18: Response Surface Graphs of Volt and Ampere on Corrosion Rate

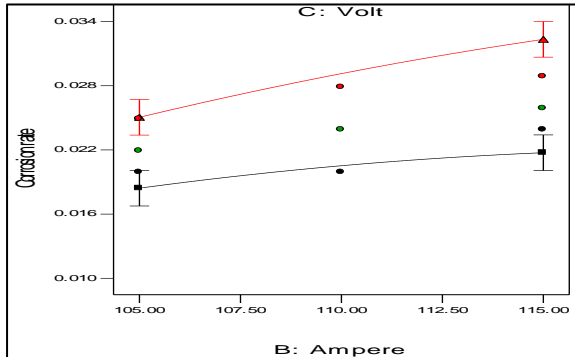


Fig 19: Optimizing FSW Process Parameters of Tool Rotational Speed and Welding Speed on Tensile Strength, Elongation and Hardness

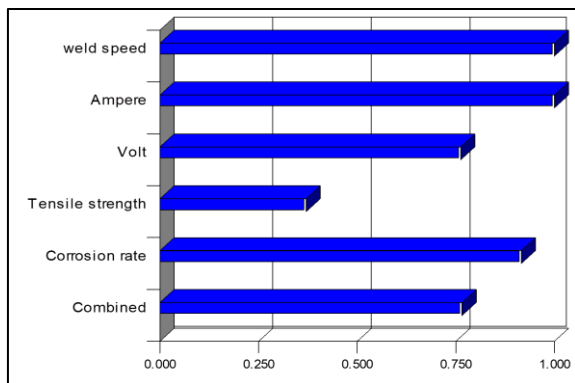


Table 8 :ANOVA Test Results for Corrosion Rate

Sources	Sum of Squares	D F	Mean Square	F Value	Prob > F	Result
Model	2.677E-003	9	2.974E-004	80.74	< 0.0001	significant
S	2.205E-004	1	2.205E-004	59.85	< 0.0001	
A	1.313E-004	1	1.313E-004	35.63	< 0.0001	
V	2.365E-004	1	2.365E-004	64.18	< 0.0001	
S ²	8.563E-005	1	8.563E-005	23.24	0.0002	
A ²	1.185E-006	1	1.185E-006	0.32	0.5780	
V ²	8.963E-006	1	8.963E-006	2.43	0.1372	
SA	1.200E-005	1	1.200E-005	3.26	0.0889	
SV	3.333E-007	1	3.333E-007	0.090	0.7672	
AV	1.200E-005	1	1.200E-005	3.26	0.0889	
Residual	6.263E-005	17	3.684E-006			
Lack of fit		17		0.71		Not significant
Pure error		0				
Cor Total	2.740E-003	26				

Table 9 :Coefficient of Determination Values for Tensile Strength and Corrosion Rate

R2	Adj R2	Pred R2	Adeq Precision
0.9771	0.9650	0.9426	30.439

3.5 Optimizing fsw process parameters

In this work, MIG process parameters were optimized using response surface methodology (RSM). For designing a set of experiments, developing a mathematical model, analyzing the optimum combination of input parameters and expressing the values graphically, RSM is most successful method [8]. To achieve the influencing temperament and optimized condition of the process parameter on tensile strength and corrosion rate, the surface plots and contour plots which are the indications of possible independence of factors have been developed for the proposed empirical relation by considering one parameter in the middle level and two parameters in the x and y axis as shown in Figures 13, 15, and 17.

These response contours can help in the prophecy of the response (tensile strength and corrosion rate) for any region of the experimental

domain [16]. Figures 14, 16 and 18 show three-dimensional response surface plots for the response.

Tensile strength and corrosion rate obtained from the regression model. The maximum achievable tensile strength values have been taken from the apex of the response plot. A contour plot is created which plays a most important role in displaying the region of the optimal process visually. Creating contour plot can be more complex for second order responses compared to the simple series of parallel lines that can occur with first order models see figure 19.

4.0 Conclusions

On the basis of experimental investigation corrosion rate and tensile strength carried out on the welded pipe of Al 6061 prepared according to MIG processes, the following conclusions are given:

1. Regression modeling equations of the similar MIG welded 6061 aluminum pipe were developed based on the experimental values of Ultimate tensile strength and corrosion rate the developed models were validated for 95% confidence level.
2. The increase in ampere and decreases in volt due to an increase in tensile strength and decrease corrosion rate.
3. The process parameters were optimized for maximum tensile strength characteristics and corrosion rate for the similar joints fabricated using MIG welding shows a reduction in filler metal.

Acknowledgement

The corresponding Author would like to express his gratitude to Eng. Hesham El-Gandy Middle Delta for Electricity Production Co. for her invaluable support in this paper.

References

- [1] C Zhou, X Yang, G Luan. Effect of Root Flaws in the Fatigue Property of Friction Stir Welds in 2024-T3 Aluminum Alloys. *Materials Science and Engineering: A*, 418(1), 2006, 155-160
- [2] TJ Lienert, WL Stellwag, BB Grimmer and RW Warke, *Friction Stir Welding Studies on Mild Steel*, *Welding Journal*, 70(13), 2003, 1-9
- [3] SY Merchant. Investigation on effect of welding current on welding speed & Hardness of HAZ & weld metal of mild steel. *International Journal of Research in Engineering & Technology*, 4(3), 2015, 44-48.
- [4] C Hamilton, S Dymek, M Blicharski. Mechanical properties of Al 6101-T6 welds by Friction stir welding and metal inert gas welding. *Archives of Metallurgy and Materials*, 52(1), 2007, 67-72
- [5] ABM M Rahman, S Kumar, AR Gerson. The role of silicon in the corrosion of AA6061 aluminium alloy laser weldments. *Corrosion Science*, 52(6), 2010, 1969-1975.
- [6] G Mathers. *The welding of aluminium and its alloys*. Florida: Woodhead Publishing Limited, 2002, 45.
- [7] A Squillace, A De Fanzo, G Giorleo, F Bellucci. A comparison between FSW and TIG welding techniques: modifications of microstructure and pitting corrosion resistance in AA 2024-T3 butt joints. *Journal of Materials Processing Technology* 152(3), 2004, 97-105.
- [8] KP Rao, N Ramanaiah, N Viswanathan. Partially melted zone cracking in AA6061 welds. *Materials and Design*, 29(1), 2008, 179-186.
- [9] J Song, SB Lin, CL Yang, CL Fan. Effects of Si addition on intermetallic compound layer of aluminium-steel TIG welding-brazing joint. *Journal of Alloys and Compounds*, 488(1), 2009, 217-222.
- [10] DD Dhancholia, A Sharma, C Vyas. Optimisation of Friction Stir Welding Parameters for AA 6061 and AA 7039 Aluminium Alloys by Response Surface Methodology (RSM). *International Journal of Advanced Mechanical Engineering*. 4(5), 2014, 565-571.
- [11] AM Khourshid, I Sabry. Analysis of welded joints using friction stir welding, metal inert gas and tungsten inert gas. *Engineering and technology in India*, 7(1), 2016, 1-7.

- [12] D Kanakaraja, P Hema, K Ravindranath. Comparative Study On Different Pin Geometries Of Tool Profile In Friction Stir Welding Using Artificial Neural Networks. *International Journal of Mechanical Engineering and Technology*, 4(2), 2013, 245-253.
- [13] AM El-Kassas, AM Khourshid, I Sabry. Integration between artificial neural network and responses surfaces methodology for modeling of friction stir welding. *Internat. J. Adv. Engg. Res. & Sci. (IJAERS)*, 2(3), 2015, 67-73.
- [14] R Palanive, PK Mathews. Prediction and optimization of process parameter of friction stir welded AA5083-H111 aluminum alloy using response surface methodology, 19(1), 2012, 1-8.
- [15] R Shanmugam, N Murugan. Effect of gas tungsten arc welding process variables on dilution and bead geometry of Stellite 6 hardfaced valve seat rings, 22(5), 2013, 375-383.
- [16] AM Khourshid, AM El-Kassas, HM Hindawy, I Sabry. Optimization of Friction Stir Welding Parameters for Joining Aluminum Pipes Using Regression Analysis. *International Journal of Civil, Mechanical and Energy Science (IJCMES)*, 2(1), 2016, 1-5.
- [17] http://cms3.minitab.co.kr/board/minitab_data/7.%20DesignofExperimentsAllTopics.pdf
- [18] KPMurali, Ramanaiah, Prasada. Optimization of process parameters for friction stir welding of dissimilar aluminum alloys AA2024T6 and AA6351T6 by using Taguchi method. *International Journal of Industrial Engineering Computations*, 4(1), 2013, 71-80.